Identifying druggable targets and preclinically overcoming non-genetic/adaptive resistance to Menin inhibitors in AML with MLL1r or mtNPM1

Warren Fiskus[1], Christopher P. Mill[1], Jessica Piel[2], Mike Collins[2], Murphy Hentemann[2], Christine E. Birdwell[1], Kaberi Das[1], John A. Davis[1], Hanxi Hou[1], Surbhi Sharma[1], Koji Sasaki[1], Sanam Loghavi[1], Branko Cuglievan[1], Gautam Borthakur[1], Tapan M. Kadia[1], Naval Daver[1], Courtney D. DiNardo[1], and Kapil N. Bhalla[1].

[1]The University of Texas MD Anderson Cancer Center, Houston, TX; [2] Foghorn Therapeutics, Cambridge, MA

THE UNIVERSITY OF TEXAS MD Anderson Cancer Center

Making Cancer History®

Introduction

Menin binds to the Menin binding domain (MBD) in the N-terminus of MLL1 (KMT2A), which is a large (3696 amino acids) transcriptional regulator and a histone-lysine-N-methyltransferase. The C-terminus of MLL1 contains the SET domain acting as a histone methyltransferase that mediates histone H3 lysine 4 trimethylation. The Menin-KMT2A complex regulates expression of the leukemogenic Homeobox A9 (HOXA9) and its co-factor MEIS1 in myeloid stem progenitor cells. In AML with MLL1 rearrangement or MLL1 fusion proteins (FP), the N-terminus of MLL1 becomes fused to over 80 partner proteins including AF4, AF9, ENL and ELL, which are part of and recruit the super elongation complex (SEC) (including AFF1/4 and pTEFb) and DOT1L to induce H3K4Me3 and H3K79Me2 marks on active chromatin. This results in an aberrant leukemic transcriptional program including dysregulated expression of HOXA9, MEIS1, PBX3, FLT3, MEF2C and CDK6. On the other hand, in mutant NPM1 AML cells, wild type MLL1 is the main regulator of HOXA9, MEIS1 and FLT3, promoting self-renewal of myeloid progenitor cells. Menin inhibitors have been developed that disrupt the binding of Menin to its binding pocket in MLL1/2 and MLL1-FP leading to reduced activity of HOXA9 and MEIS1 and repression of MLL1 or MLL1-FP target genes. Clinical trials have demonstrated that Menin inhibitors (MI) are well-tolerated and clinical remissions have been observed in patients with relapsed/refractory AML harboring MLLr or mtNPM1. Unfortunately, most patients either fail to respond or eventually relapse. MI-resistance in AML with MLL1r or mtNPM1 is either due to recently described hotspot mutations in the MI-binding domain of Menin or in approximately two-thirds of cases is non-genetic and adaptive, due to a dysregulated epigenome, transcriptome, and proteome.

In the present studies, through repeated shocks with LD_{90} dosing of Menin inhibitor SNDX-50469, followed by drug washout and recovery, we have generated MLL1r (MV4-11-MITR) and mtNPM1 (OCI-AML3-MITR) AML cell lines that are tolerant/resistant (TR) to MI with LD_{50} values greater than 1 μM. Utilizing whole exome sequencing, we confirmed that these cells were lacking in new driver mutations. We also determined that the resistance in the MITR cells was not due to the presence of any of the recently described hotspot mutations in Menin. ChIP-Seq analysis of H3K27Ac showed that the activities of super enhancers and core transcriptional regulatory circuitry was reduced in the MITR cell types. Non-genetic/adaptive resistance to Menin inhibitor also concordantly reduced genome-wide ATAC-Seq and RNA-Seq peaks in the OCI-AML3-MITR cells with significant depletion of MEIS1, IGF2BP2, BCL2, and PBX3, with concomitant induction of leukemia stem cell associated CLEC12A and CD244 expressions. We conducted a epigenetic target focused domain-specific CRISPR screen in MV4-11-MITR cells. This screen identified several druggable co-dependencies (e.g. EP300 and MOZ) and co-enrichments (SMARCA4, CREBBP and BRD4) with MI, suggesting them as potential mechanisms of non-genetic/adaptive MI resistance. Consistent with these findings, co-treatment with SMARCA2/SMARCA4 (chromatin remodeler ATPases) inhibitor FHD-286 and the BETi OTX015 or the MI SNDX-50469 exerted synergistic lethality in MV4-11-MITR and OCI-AML3-MITR cells as well as in PD MITR AML cells with MLL1r or mtNPM1. Co-treatment with CBP/p300 inhibitor GNE049 or GNE781 was also synergistic with MI in these cells. In vivo treatment with FHD-286 and SNDX-5613 or OTX015 significantly reduced the AML burden and markedly improved the median and overall survival of NSG mice bearing OCI-AML3-MITR xenografts. Similar reduction in leukemia burden and improvement in survival was also observed in a Menin inhibitor refractory/resistant MLL1r AML PDX treated with SNDX-5613 and FHD-286 or OTX015 plus FHD-286. These findings underscore preclinical activity of epigenetically-targeted agent-based combinations and highlight their promise in overcoming MI resistance in AML with MLL1r or mtNPM1.

Results

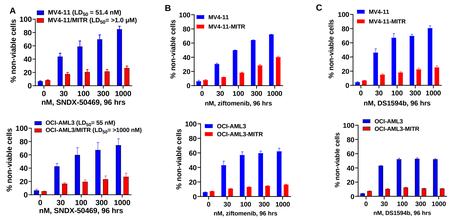

D

Drug	LD_{50} value (in nM)			
	MV4-11	MV4-11-MITR	OCI-AML3	OCI-AML3-MITR
ziftomenib	122.67	>1000	76.77	>1000
DS1594b	32.67	>1000	122.14	>1000

Figure 1. Compared to parental MV4-11 and OCI-AML3 cells, MV4-11-MITR and OCI-AML3-MITR cells exhibit in vitro cross resistance to Menin inhibitors ziftomenib and DS1594b. A-D. MV4-11, MV4-11-MITR, OCI-AML3, and OCI-AML3-MITR cells were treated with the indicated concentrations of SNDX-50469, ziftomenib (KO-539) or DS1594b for 96 hours. At the end of treatment, cells were stained with TO-PRO-3 iodide and the percentages of non-viable cells were determined by flow cytometry. LD_{50} values were calculated utilizing CompuSyn software.

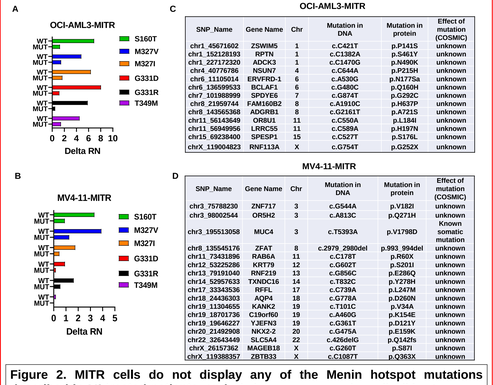

C

SNP_Name	Gene Name	Chr	Mutation in DNA	Mutation in protein	Effect of mutation (COSMIC)
chr1_45671602	ZSWIM5	1	c.C421T	p.P141S	unknown
chr1_152128193	RPTN	1	c.C1382A	p.S461Y	unknown
chr1_227127320	ADCK3	1	c.C1470G	p.N490K	unknown
chr4_40776786	NSUN7	4	c.C644A	p.P215H	unknown
chr6_11105014	ERVFRD-1	6	c.A530G	p.N177Ss	unknown
chr8_136599533	BCLAF1	6	c.G480C	p.Q160H	unknown
chr7_101988999	SPDYE6	7	c.G874T	p.G292C	unknown
chr8_21959744	FAM150B2	8	c.A1910C	p.H637P	unknown
chr8_143565368	ADGRB1	8	c.G2161T	p.A721S	unknown
chr11_56143649	ORBU1	11	c.C550A	p.L184I	unknown
chr11_56949956	LRRC55	11	c.C589A	p.H197N	unknown
chr15_69238400	SPESP1	15	c.C527T	p.S176L	unknown
chrX_119004823	RNF113A	X	c.G754T	p.G252X	unknown

MV4-11-MITR

SNP_Name	Gene Name	Chr	Mutation in DNA	Mutation in protein	Effect of mutation (COSMIC)
chr3_75788230	ZNF717	3	c.G544A	p.V182I	unknown
chr3_98002544	ORS8I2	3	c.A813G	p.Q271H	unknown
chr3_195513058	MUC4	3	c.T5393A	p.V1798D	Known somatic mutation
chr8_135545176	ZFAT	8	c.2979_2980del	p.993_994del	unknown
chr11_734318896	RABEA	11	c.C178T	p.R60X	unknown
chr12_53225286	KRT79	12	c.G602T	p.S201I	unknown
chr13_79191040	RNF219	13	c.G856C	p.E286Q	unknown
chr14_52957633	TXNDC16	14	c.T832C	p.Y278H	unknown
chr17_33343536	RFFL	17	c.C739A	p.L247M	unknown
chr18_24436303	AQP4	18	c.G778A	p.D260N	unknown
chr19_11304655	KANK2	19	c.T101C	p.V34A	unknown
chr19_18701736	C19orf60	19	c.A460G	p.K154E	unknown
chr19_19646227	YJEFN3	19	c.G361T	p.D121Y	unknown
chr20_21492908	NKX2-2	20	c.G475A	p.E159K	unknown
chr22_32643449	SLC5A4	22	c.42fs6delG	p.Q142fs	unknown
chrX_26157362	MAGEB18	X	c.G260T	p.S87I	unknown
chrX_133388357	ZBTB33	X	c.C1087T	p.Q363X	unknown

Figure 2. MITR cells do not display any of the Menin hotspot mutations described in MI-treated patients, and whole exome sequencing cells did not uncover new driver mutations or genetic mechanisms of resistance in OCI-AML3-MITR and MV4-11-MITR cells. **A-B**. Genomic DNA was isolated from OCI-AML3-MITR and MV4-11 MITR cells and utilized with custom TaqMan assays for detecting hotspot mutations in Menin. **C-D**. OCI-AML3, OCI-AML3-MITR, MV4-11 and MV4-11-MITR cells in log phase were harvested and genomic DNA was isolated and subjected to whole exome sequencing. The tables show novel mutations that were identified in the OCI-AML3-MITR and MV4-11 MITR cells compared to their respective parental control cells. The mutation in the DNA and the resulting mutation in the protein are shown as well as any known effect of the mutation from the COSMIC database.

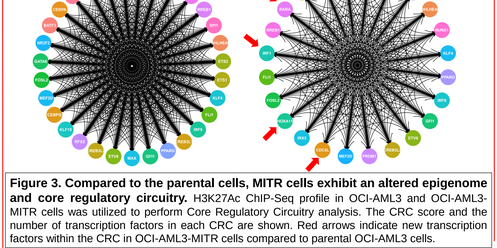

Figure 3. Compared to the parental cells, MITR cells exhibit an altered epigenome and core regulatory circuitry. H3K27Ac ChIP-Seq profile in OCI-AML3 and OCI-AML3-MITR cells was utilized to perform Core Regulatory Circuitry analysis. The CRC score and the number of transcription factors in each CRC are shown. Red arrows indicate new transcription factors within the CRC in OCI-AML3-MITR cells compared to parental OCI-AML3 cells.

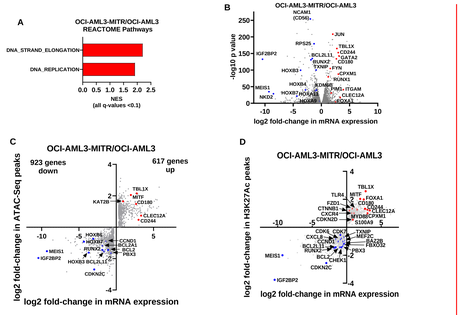

Figure 4. OCI-AML3-MITR cells exhibit concordant alterations in H3K27Ac ChIP-Seq occupancy and RNA-Seq expression with significant induction in the normalized enrichment scores for REACTOME_DNA_REPLICATION and DNA_STRAND_ELONGATION genes and increased expression of CLEC12A and FOXA1. A-B. OCI-AML3 and OCI-AML3-MITR cells in exponential phase were harvested and utilized for RNA-Seq analysis. Differential expression analyses were conducted on the RNA-Seq (volcano plot) and gene set enrichment analysis was performed compared to REACTOME pathways. **C-D**. Scatterplot of log2 fold-changes in concordant ATAC-Seq peaks and RNA-Seq expression alterations or H3K27Ac ChIP-Seq peaks and RNA-Seq-determined mRNA expression alterations in OCI-AML3-MITR versus OCI-AML3 parental cells.

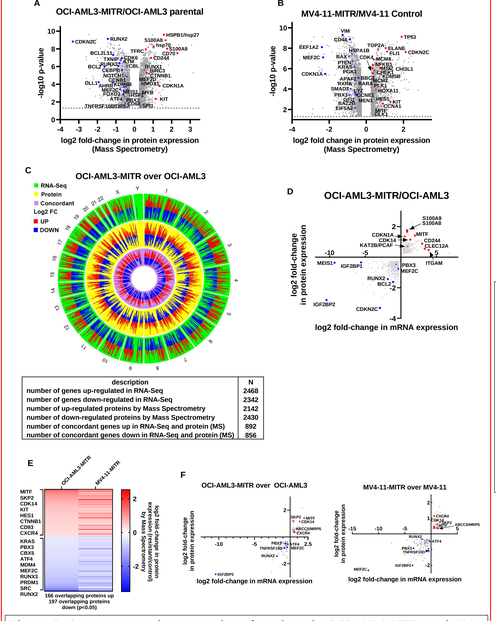

description	N
number of genes up-regulated in RNA-Seq	2468
number of genes down-regulated in RNA-Seq	2342
number of up-regulated proteins by Mass Spectrometry	2142
number of down-regulated proteins by Mass Spectrometry	2430
number of concordant genes up in RNA-Seq and protein (MS)	892
number of concordant genes down in RNA-Seq and protein (MS)	856

Figure 5. Common protein expression alterations in OCI-AML3-MITR and MV4-11-MITR compared to parental cells determined by mass spectrometry analysis. A-B. MV4-11, MV4-11-MITR, OCI-AML3, and OCI-AML3-MITR cells in exponential phase were utilized for whole proteome mass spectrometry analyses. Volcano plots (log2 fold-change versus -log10 p-value) of mass spectrometry-determined protein expression changes in OCI-AML3-MITR over OCI-AML3 and MV4-11-MITR over MV4-11 cells are shown. **C-D**. Circos plot and scatterplot of significantly altered and concordant mRNA and protein expression changes in OCI-AML3-MITR over OCI-AML3 cells. The table indicates the number of concordant up and down regulated mRNA and protein changes in the MITR cells versus the parental cells. **E**. Heat map of common (overlapping) and significant protein expression changes in OCI-AML3-MITR and MV4-11-MITR cells (166 common up; 197 common down; p< 0.05). **F**. Scatterplot of log2 fold-changes of selected, common, concordant mRNA and protein expression alterations in OCI-AML3-MITR over OCI-AML3 and MV4-11-MITR over MV4-11 cells.

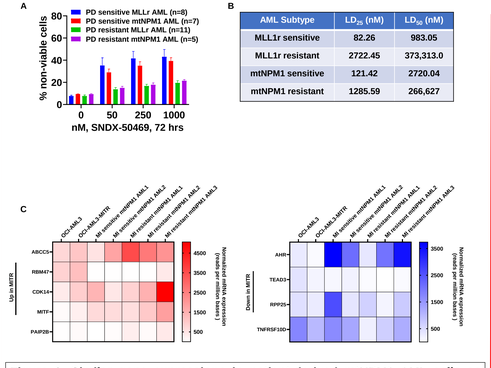

AML Subtype	LD_{25} (nM)	LD_{50} (nM)
MLL1r sensitive	82.26	983.05
MLL1r resistant	2722.45	373,313.0
mtNPM1 sensitive	121.42	2720.04
mtNPM1 resistant	1285.59	266,627

Figure 6. Similar gene expressions in patient-derived mtNPM1 AML cells as those identified in OCI-AML3-MITR cells. **A-B**. Patient-derived MLL1r and mtNPM1 AML cells were treated with the indicated concentrations of SNDX-50469 for 72 hours. The % non-viable cells were determined by staining with TO-PRO-3 iodide and flow cytometry. Samples were classified as Menin inhibitor sensitive or resistant based on their LD25 and LD50 values. **C**. Heat map of overlapping normalized gene expressions determined by RNA-Seq analysis in OCI-AML3, OCI-AML3-MITR and five patient-derived mtNPM1 expressing AML samples. Genes listed are those which are increased or decreased in MITR cells and MI-resistant PD mtNPM1 AML cells.

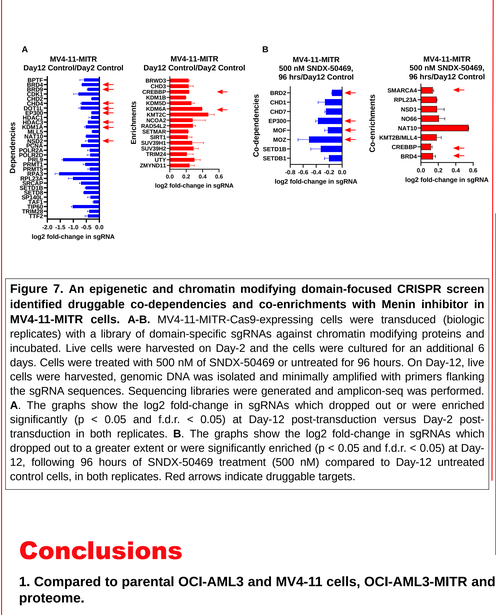

Figure 7. An epigenetic and chromatin modifying domain-focused CRISPR screen identified druggable co-dependencies and co-enrichments with Menin inhibitor in MV4-11-MITR cells. A-B. MV4-11-MITR-Cas9-expressing cells were transduced (biologic replicates) with a library of domain-specific sgRNAs against chromatin modifying proteins and incubated. Live cells were harvested on Day-2 and the cells were cultured for an additional 6 days. Cells were treated with 500 nM of SNDX-50469 or untreated for 96 hours. On Day-12, live cells were harvested, genomic DNA was isolated and minimally amplified with primers flanking the sgRNA sequences. Sequencing libraries were generated and amplicon-seq was performed. **A**. The graphs show the log2 fold-change in sgRNAs which dropped out or were enriched significantly ($p < 0.05$ and f.d.r. < 0.05) at Day-12 post-transduction versus Day-2 post-transduction in both replicates. **B**. The graphs show the log2 fold-change in sgRNAs which dropped out to a greater extent or were significantly enriched ($p < 0.05$ and f.d.r. < 0.05) at Day-12, following 96 hours of SNDX-50469 treatment (500 nM) compared to Day-12 untreated control cells, in both replicates. Red arrows indicate druggable targets.

Conclusions

1. Compared to parental OCI-AML3 and MV4-11 cells, OCI-AML3-MITR and MV4-11-MITR cells exhibit an altered epigenome, transcriptome and proteome.

2. A CRISPR gRNA screen identified co-dependencies (BRD2, EP300, and MOZ) and co-enrichments (SMARCA4, CREBBP, and BRD4) with MI in MV4-11 MITR cells.

3. Co-treatment with FHD-286, OTX015, or HAT (CBP/p300) inhibitor GNE781 and SNDX-50469 exerted synergistic lethality in MV4-11-MITR and OCI-AML3-MITR cells as well as in PD, MITR AML cells with MLL1r or mtNPM1.

4. Compared to treatment with FHD-286, OTX015, SNDX-5613 alone or vehicle control, co-treatment with FHD-286 and OTX015 or SNDX-5613 reduced AML burden and significantly improved survival of mice bearing OCI-AML3-MITR xenografts and MI-tolerant MLL1r AML PDX cells.

5. These findings demonstrate the pre-clinical efficacy of rational combinations of MI with BETi, HATi or FHD-286 to overcome MI tolerance/resistance and underscores their promise against MI-resistant AML with MLL1r or mtNPM1.

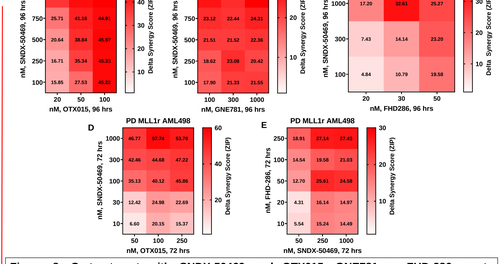

Figure 8. Co-treatment with SNDX-50469 and OTX015, GNE781 or FHD-286 exerts synergistic lethal activity against OCI-AML3-MITR and patient-derived MLL1r AML cells exhibiting ex vivo resistance to MI treatment. A-E. OCI-AML3-MITR and PD MLL1r AML (ex vivo resistant to MI) cells were treated with the indicated concentrations of SNDX-50469 and/or OTX015, GNE781 or FHD-286 for 72-96 hours. At the end of treatment, cells were stained with TO-PRO-3 iodide and the % non-viable cells were determined by flow cytometry. Delta synergy scores were determined by the ZIP method utilizing the SynergyFinder web application. Synergy scores >1.0 indicate a synergistic interaction of the two agents in the combination.

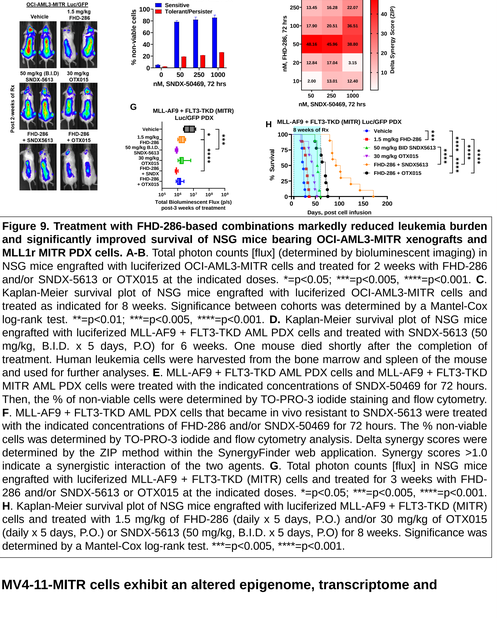

Figure 9. Treatment with FHD-286-based combinations markedly reduced leukemia burden and significantly improved survival of NSG mice bearing OCI-AML3-MITR xenografts and MLL1r MITR PDX cells. A-B. Total photon counts [flux] (determined by bioluminescent imaging) in NSG mice engrafted with luciferized OCI-AML3-MITR cells and treated for 2 weeks with FHD-286 and/or SNDX-5613 or OTX015 at the indicated doses. *=p<0.05; ***=p<0.005, ****=p<0.001. **C**. Kaplan-Meier survival plot of NSG mice engrafted with luciferized OCI-AML3-MITR cells and treated as indicated for 8 weeks. Significance between cohorts was determined by a Mantel-Cox log-rank test. **=p<0.01; ***=p<0.005, ****=p<0.001. **D.** Kaplan-Meier survival plot of NSG mice engrafted with luciferized MLL-AF9 + FLT3-TKD AML PDX cells and treated with SNDX-5613 (50 mg/kg, B.I.D. x 5 days, P.O) for 6 weeks. One mouse died shortly after the completion of treatment. Human leukemia cells were harvested from the bone marrow and spleen of the mouse and used for further analyses. **E**. MLL-AF9 + FLT3-TKD AML PDX cells and MLL-AF9 + FLT3-TKD MITR AML PDX cells were treated with the indicated concentrations of SNDX-50469 for 72 hours. Then, the % of non-viable cells were determined by TO-PRO-3 iodide staining and flow cytometry. **F**. MLL-AF9 + FLT3-TKD AML PDX cells that became in vivo resistant to SNDX-5613 were treated with the indicated concentrations of FHD-286 and/or SNDX-50469 for 72 hours. The % non-viable cells was determined by TO-PRO-3 iodide and flow cytometry analysis. Delta synergy scores were determined by the ZIP method within the SynergyFinder web application. Synergy scores >1.0 indicate a synergistic interaction of the two agents. **G**. Total photon counts [flux] in NSG mice engrafted with luciferized MLL-AF9 + FLT3-TKD (MITR) cells and treated for 3 weeks with FHD-286 and/or SNDX-5613 or OTX015 at the indicated doses. *=p<0.05; ***=p<0.005, ****=p<0.001. **H**. Kaplan-Meier survival plot of NSG mice engrafted with luciferized MLL-AF9 + FLT3-TKD (MITR) cells and treated with 1.5 mg/kg of FHD-286 (daily x 5 days, P.O.) and/or 30 mg/kg of OTX015 (daily x 5 days, P.O.) or SNDX-5613 (50 mg/kg, B.I.D. x 5 days, P.O) for 8 weeks. Significance was determined by a Mantel-Cox log-rank test. ***=p<0.005, ****=p<0.001.

Poster Session Online

Scan the QR code to view this poster on a mobile device.

American Society of Hematology
Helping hematologists conquer blood diseases worldwide

604. Molecular Pharmacology and Drug Resistance: Myeloid Neoplasms: Poster I

Warren C. Fiskus

SAT-1373

ASH2024